

# Band Pass Filter Bank Design (250–500 MHz) for Radio Astronomy Application Based on Metamaterial ZOR Techniques

**Sougata Chatterjee, Anil Raut, Suresh Kumar**  
**Front End Group, Giant Metrewave Radio Telescope**  
**Pune, India**

## INTRODUCTION

Metamaterial (MTM) is an artificial composite material for which we can change its electromagnetic properties [1]. The equivalent circuit approach of MTM was developed by Caloz and Itoh [2] and Sanada et al. [3], and this approach has led to the concept of composite right- and left-handed (CRLH) materials. This concept fully takes into account the parasitic right-handed (RH) effects, which is unavoidable in a practical application. The zeroth-order resonator (ZOR) has the mode number zero, and its resonator length is invariant of its wavelength. Sanada et al. [3] first proposed MTM-ZOR and realized it in microstrip configuration. Using the MTM-ZOR technique, several researchers [4]–[8] have designed band pass filters (BPFs) in different frequency bands.

The Giant Metrewave Radio Telescope (GMRT) is the world's largest meter wavelength radio telescope (see Swarup et al. [10]). In the current upgrade of the GMRT receiver system (250–500 MHz) we have redesigned BPFs using MTM-ZOR techniques in the following bands: 240–340, 300–400, 360–460, and 420–520 MHz (6-dB bandwidth). A literature survey shows that low-frequency design within a constrained size has not been previously attempted. This article describes briefly a unit cell of MTM-ZOR and proceeds further into the design of a five-pole BPF at a 420–520 MHz band. Using a parametric approach, our designs were optimized to obtain a good bandwidth and good roll-off response. The simulation was carried out using method of moments ADS-2013 software. The fabricated BPF was installed in the upgraded GMRT system [11].

## MTM-ZOR BPF DESIGN FOR 420–520 MHz

The unit cell of a MTM transmission line (TL) is a series consisting of a shunt capacitor ( $C_L$ ) and an inductor ( $L_L$ ), where the

Authors' current address: S. Chatterjee, A. Raut, S. Kumar, Front End Group, Giant Metrewave Radio Telescope (GMRT), NCRA-TIFR, Pune-410504, India, E-mail: (sougata.sameer@gmail.com).

Manuscript received October 24, 2014, and ready for publication December 16, 2014.

DOI No. 10.1109/MAES.2015.140072.

Review handled by M. De Santos.

0885/8985/15/\$26.00© 2015 IEEE

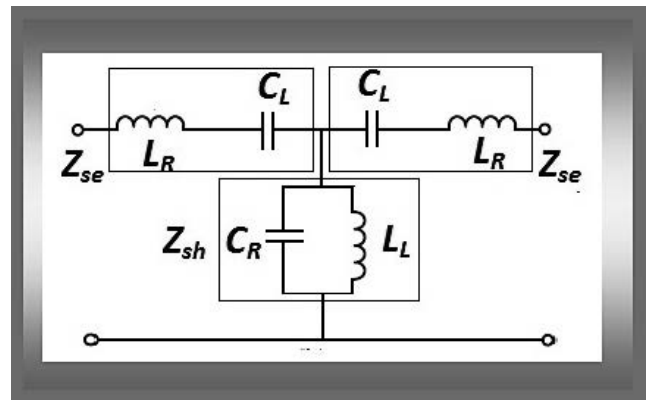


**Figure 1.**  
Unit cell model of MTM-TL.

propagation constant ( $\beta$ ) is negative in a specific frequency band (Figure 1). This type of TL is called a periodically left-handed transmission line (PLTL). Parasitic RH effects hamper the designing of a pure PLTL; hence, the MTM loaded line is called a CRLH TL [6], [7].

In the CRLH TL, the resonance conditions are as follows:

$$f_L = \frac{1}{2\pi\sqrt{L_L C_L}}, f_R = \frac{1}{2\pi\sqrt{L_R C_R}} \quad (1)$$

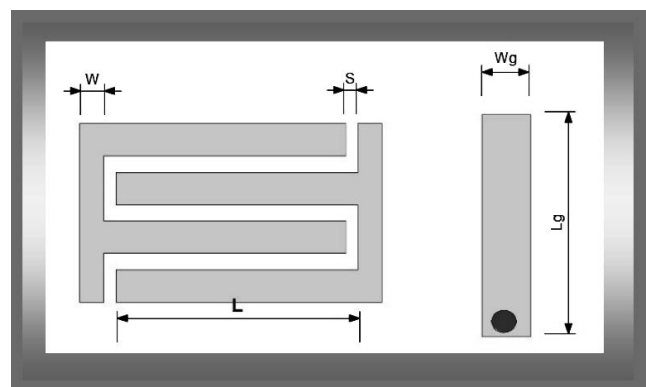
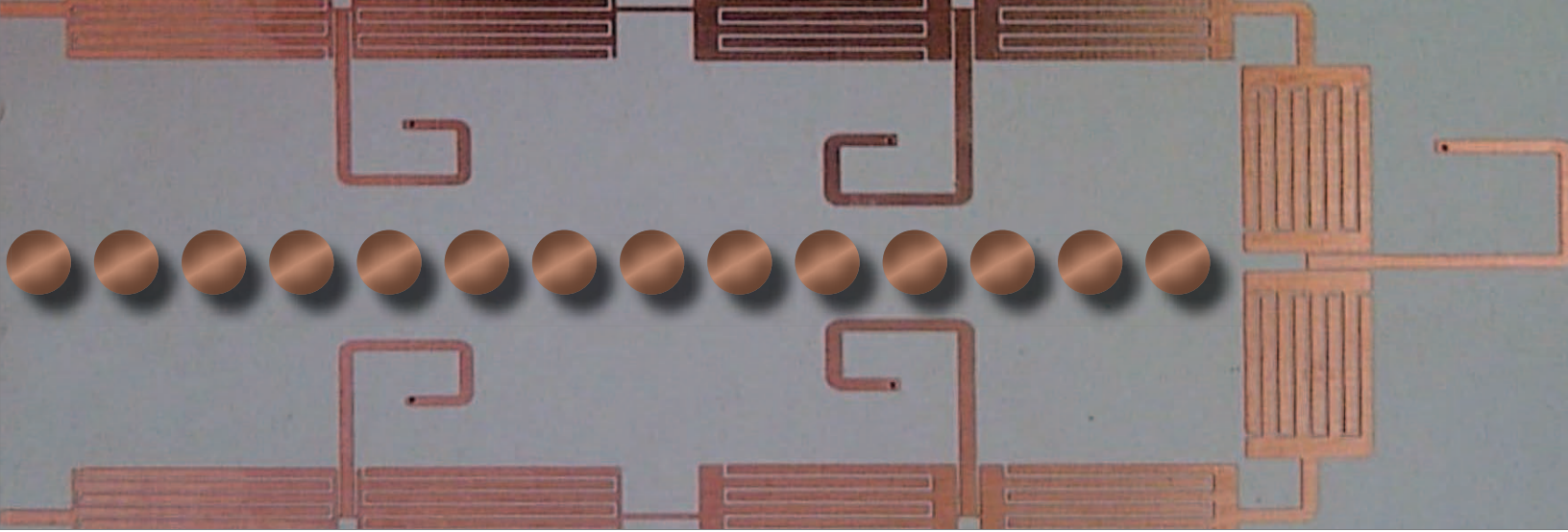


**Figure 2.**  
Interdigital capacitor with grounded stub.



$$f_{se} = f_{sh} = f_o, f_0 = \sqrt{f_L f_R} \quad (2)$$

$$f_{se} = \frac{1}{2\pi\sqrt{L_R C_L}}, f_{sh} = \frac{1}{2\pi\sqrt{L_L C_R}} \quad (3)$$

Here,  $f_{se}$ ,  $f_{sh}$ ,  $f_L$ ,  $f_R$ , and  $f_o$  correspond to the series resonance point, shunt resonance point, lower band edge, upper band edge, and center frequency, respectively. At a balance condition,  $f_{se}$  is equal to  $f_{sh}$  [7].

For making a microstrip-based MTM-ZOR unit cell, the interdigital capacitor can be utilized as the series capacitor and the ground stub can be used as the shunt inductor. Moreover, a higher capacitor value is a smaller area that can be achieved if an interdigital capacitor is used. Figure 2 shows the interdigital capacitor and grounded stub. The governing equations are [9]

$$C(pF) = \frac{\epsilon_{re} 10^{-3}}{18\pi} \frac{K(k)}{K'(k)} (n-1)L \quad (4)$$

where  $n$  is the number of fingered interdigital lines,  $L$  is the length of the finger, and  $K$  and  $K'$  are the complete elliptical integral of the first kind and its complements, respectively.

$$K(k) = \int_0^{2\pi} \frac{d\theta}{\sqrt{1-k^2 \sin^2 \theta}} \quad (5)$$

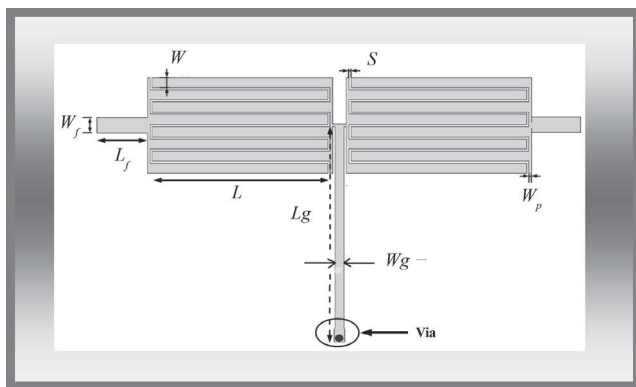


**Figure 3.** Equivalent microstrip model MTM-TL.

$$K'^2(k) = 1 - K^2(k) \quad (6)$$

$$k = \tan^2\left(\frac{a\pi}{4b}\right), a = \frac{W}{2}, b = \frac{W+S}{2} \quad (7)$$

where  $W$  and  $S$  are the finger width and the spacing between two adjacent fingers, respectively (Figure 2). Similarly, the shunt inductor of grounded stub can be represented as

$$L_L(nH) = 2 \times 10^{-4} L_g \left[ \ln\left(\frac{L_g}{W_g + t}\right) + 1.193 + 0.2235 \frac{W_g + t}{L_g} \right] k_g \quad (8)$$

where

$$k_g = 0.57 - 0.145 \ln \frac{W_g}{h} \text{ if } \frac{W_g}{h} > 0.05, \quad (9)$$

and where  $h$  is the height of the substrate and  $t$  is the metal thickness of the substrate (Figure 2). The equivalent circuit model of the MTM-ZOR microstrip form is given in Figure 3.

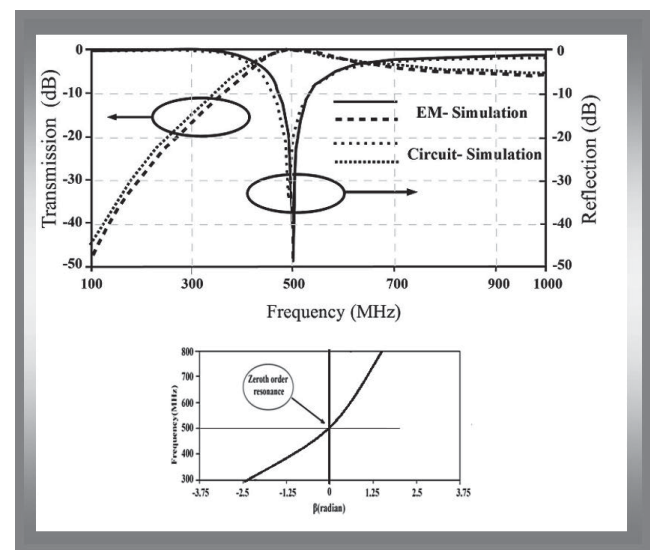


**Figure 4.** Scattering parameter and dispersion curve of CRLH unit cell.

Table 1.

Specifications for Five-Pole Filter for 420–520 MHz	
Item	Specification
Central frequency( $f_0$ )	470 MHz
Bandwidth (6dB)	100 MHz
Insertion loss	< 3 dB
Return loss in the pass band	$\geq 10$ dB
Sharp skirt (Attenuation at $f_{ue} + 30$ MHz)	$\geq 20$ dB

For making 500 MHz (center frequency) of MTM-ZOR response, the geometric information of single unit cell values is  $W = 1$  mm,  $L = 10$  mm, and  $S = 0.3$  mm and the number of the interdigital line is  $n = 8$ ; in addition,  $Wg = 0.7$  mm,  $Lg = 21$  mm, and via = 0.3 mm (diameter). The value of series capacitor  $C_L$  is 4 pF, the series inductor  $L_R$  is 0.25  $\mu$ H, the shunt inductor  $L_L$  is 0.6 nH, and the shunt capacitor  $C_R$  is 1.6 nF.

Using these specifications, we designed a microstrip based unit cell (MTM-ZOR). Its unit cell scattering parameter and dispersion ( $\omega/\beta$ ) curves are given in Figure 4.

After getting the response of a single unit cell, we designed a five-pole filter for 420–520 MHz using these techniques to meet the specifications in Table 1. For making a BPF, the individual unit of MTM-ZOR was made, after which five units were connected to the interring coupler (IRC). The IRC forms the bridge between two successive MTM-ZOR cells. The schematic figure of resonators connected with the IRC is given Figure 5.

The EM simulated structure and its fabricated design are given Figures 6A and 6B, respectively. For fabricating our prototype, we used RT/duroid 6010; the height of the substrate was 1.27 mm, and the metal thickness was 35  $\mu$ m.

The dimensions of this left-handed Maxwell (LHM)-ZOR filter are 52.1  $\times$  29 mm. Figure 7 shows the simulation results and the measured ones. The discrepancy between those two results could be attributed to variation of the substrate dielectric con-

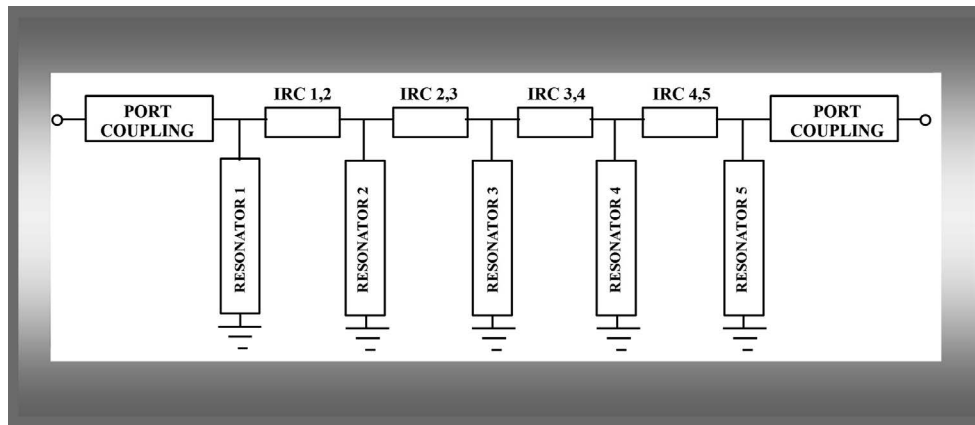


Figure 5. IRC of a pair of MTM-ZOR unit cells.

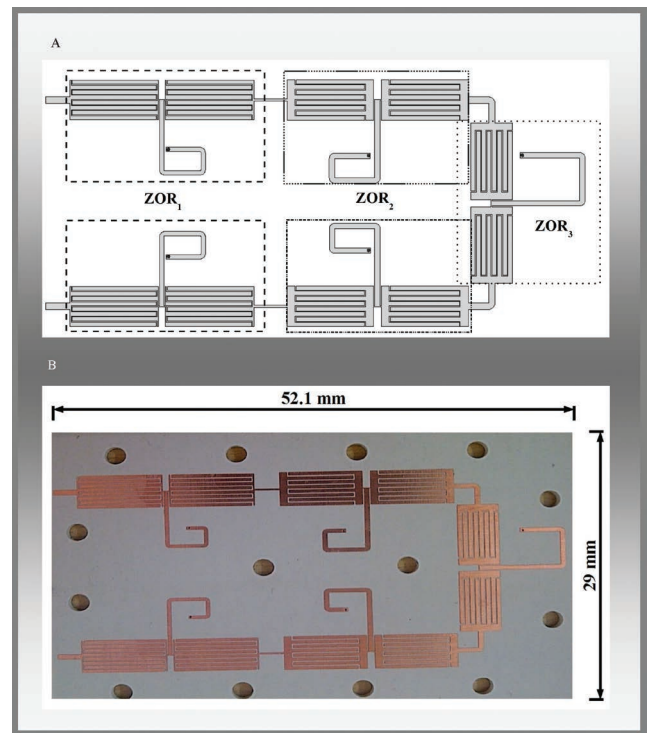


Figure 6. Compact five-pole CRLH-ZOR filter. (A) EM simulation. (B) Fabricated design.

stant and its thickness. Before designing for improved in-band response, the relationship between the high-frequency roll-off and the bandwidth is examined in the next section.

### BPF BANDWIDTH AND ROLL-OFF CONTROL

The MTM-ZOR BPF is a combination of interdigital capacitor and shorted strips. The interdigital capacitor is a combination of multiple parallel plate capacitors in series. Closely coupled capacitors improve the band width, and the high-frequency side roll-off becomes slower. The inverse behavior is seen on loosely coupled capacitors. Applying the same principle in the GMRT filter, the

gap length was increased from 0.1 to 0.25 mm, resulting in bandwidth decrease while the high-frequency side roll-off becomes sharper (Figure 8).

For making a compact BPF, we added a stub inductor inside that causes a coupling effect between two opposite inductors. The parametric study shows the different gap lengths ( $L_1, L_2, L_3$ ) that control the high-frequency side roll-off. Figure 9 shows the different gap lengths and the high-frequency side roll-off effects on the filter response.

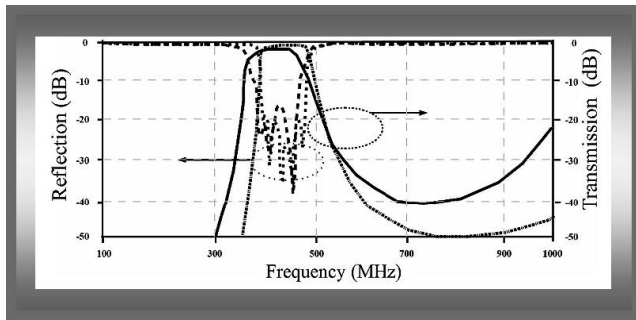


**Figure 7.** Simulated and experimental results of the LHM-ZOR-based BPF ( $S_{11}$ ,  $S_{21}$ ).

This study shows that higher-frequency roll-off and bandwidth cannot be achieved at the same time and necessitates a technical compromise. For GMRT application, bandwidth (100 MHz) is more important than higher-frequency side roll-off selectivity.

### MTM-ZOR-BASED FILTER BANK DESIGN

At the start, a MTM-ZOR BPF was designed and fabricated. Based on the results of the previous section, the filter was modified in the frequency range of 420–520 MHz. Filter design dimensions are given in Table 2. The fabricated design and its experimental results are given in Figure 10 (Table 3).

After achieving the in-band response of the 420–520 MHz subband filter, other subband filters were designed for 240–340,

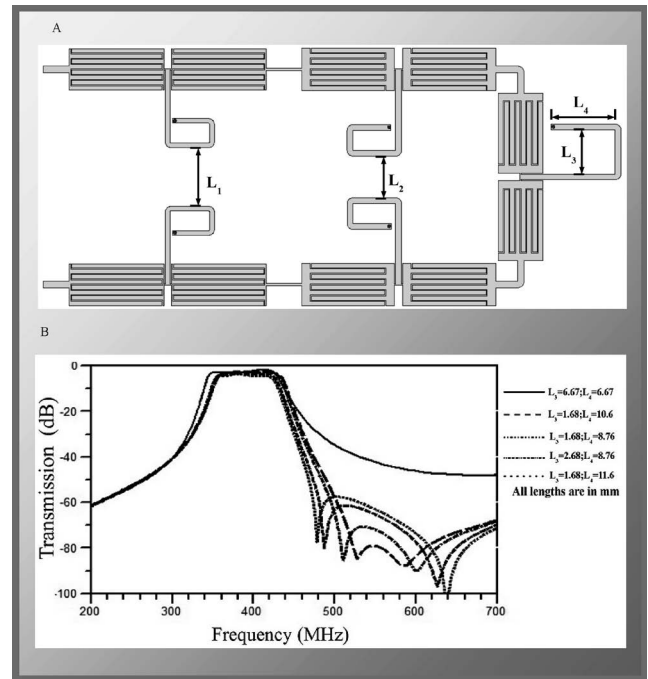


**Figure 9.** Arrangement of the gap between inductor effects on the MTM-ZOR BPF. (A) Schematic view. (B) Simulated results.

300–400, and 360–460 MHz. The design dimensions for all four subbands are given in Table 4.

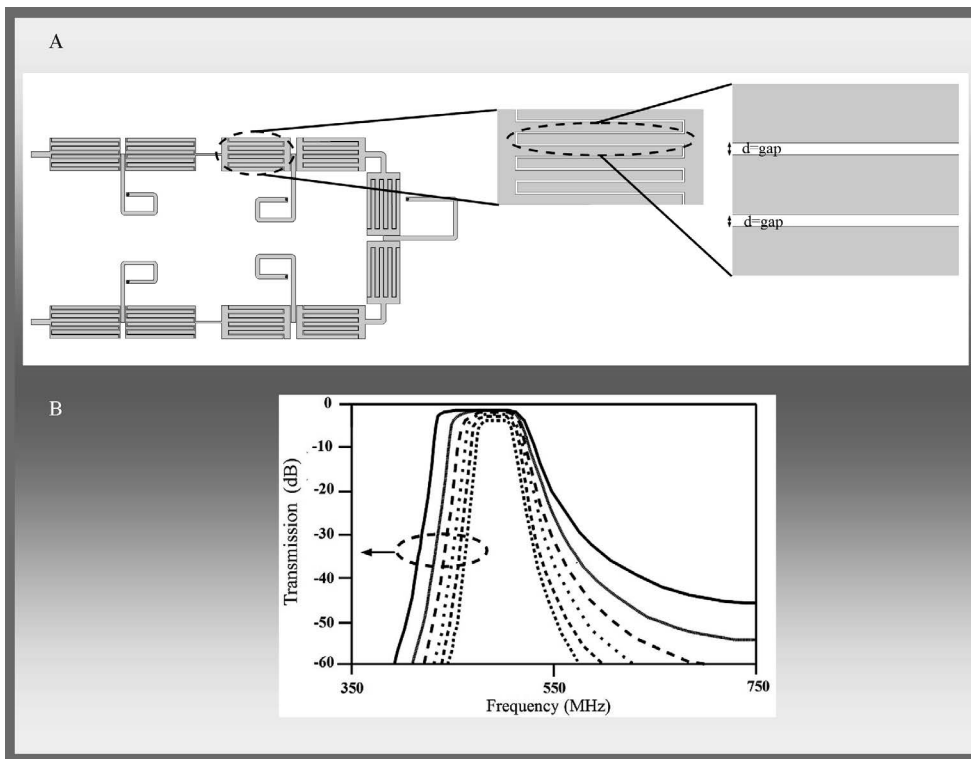


**Figure 8.** Increasing the gap length affects the MTM-ZOR BPF characteristics. (A) Schematic view. (B) Simulated results.

At lower-frequency band filters, the percentage of bandwidth is greater compared to that of the higher-frequency ones. To achieve more percentage bandwidth, the interdigital capacitor gap was trimmed. In the low-frequency band (240–340 MHz), the gap of the finger should be 0.075 mm to achieve 100 MHz of bandwidth, but commercial fabrication accuracy is in the range of 0.1 mm. Hence, we could not achieve 100 MHz of bandwidth (Table 5).

The fabricated filters of the three other subbands are shown in Figure 11. The measured results are given in Figure 12 (Table 5). The measured results closely match the desired response.

### SIZE REDUCTION OF FILTER USING MTM-ZOR

The conventional microstrip BPFs are coupled line filter, hair-pin filter, etc. In general, the par-

**Table 2.**

Design Dimensions of the Filter After Modification to the Frequency Range of 420–520 MHz (All Dimensions Are in Millimeters)		
	Design Parameter	420-520 MHz
ZOR-1	$W, S, W_p, L$	0.527, 0.11, 0.125, 8.7595
	$W_F, L_F$	0.8, 5.6
	$L_{s1}, L_{s2}, I_{s3}, I_{s4}, W_s$	8.01, 4.005, 2.0025, 2.0035, 0.555
	$L_{IRC}, W_{IRC}$	3.1, 0.3
ZOR-2	$W, S, W_p, L$	0.562, 0.11, 1.35, 6.52
	$L_{s1}, L_{s2}, L_{s3}, I_{s4}, W_s$	8.9957, 4.49785, 2.248925, 2.248925, 0.69
	$L_{IRC}, W_{IRC}$	2.5, 0.7
ZOR-3	$W, S, W_p, L$	0.585, 0.11, 1.21, 6
	$L_{s1}, L_{s2}, L_{s3}, W_s$	9.9546, 4.9773, 4.9773, 0.69
	$L_{IRC}, W_{IRC}$	2.5, 0.7

**Table 3.**

Fabricated Design of the Modified Filter and Its Experimental Results		
Design Parameter	Expected	Achieved
Band width (6 dB)	420–520 MHz	411–517 MHz
Insertion loss	–2.0–3.0 dB (470 MHz)	–2 dB (470 MHz)
Return loss	–10 dB over the band	–10 dB over the band
Higher frequency cutoff +30MHz	–30 dB (550 MHz)	–32 dB (547MHz)

**Table 4.**

Design Dimensions for the Four Subband Filters That Were Fabricated (All Dimensions Are in Millimeters)					
		420–520 MHz	360–460 MHz	300–400 MHz	240–340 MHz
ZOR-1	$W, S, W_p, L$	0.527, 0.11, 0.125, 8.7595	0.54, 0.11, 0.16, 10.5	0.587, 0.1, 0.165, 11.9	5.45, 0.1, 0.267, 18.364
	$W_F, L_F$	0.8, 5.6	4.5, 0.8	0.9, 5	0.8, 5
	$L_{s1}, L_{s2}, I_{s3}, I_{s4}, W_s$	8.01, 4.005, 2.0025, 2.0035, 0.555	8.854, 4.4595, 2.22745, 2.22745, 0.555	9.85, 4.925, 2.4625, 2.4625, 0.555	10.85, 5.425, 2.7125, 2.7125, 0.555
	$L_{IRC}, W_{IRC}$	3.1, 0.3	4.1, 0.3	4.2, 0.2	4.2, 0.2
ZOR-2	$W, S, W_p, L$	0.562, 0.11, 1.35, 6.52	0.555, 0.11, 1, 8.67	0.571, 0.1, 0.9, 9.5	0.55, 0.1, 1.1, 14.6
	$L_{s1}, L_{s2}, L_{s3}, I_{s4}, W_s$	8.9957, 4.49785, 2.248925, 2.248925, 0.69	9.8341, 4.9701, 2.4585, 2.4583, 0.69	11.35, 5.675, 2.8375, 2.8375, 0.69	12.35, 6.175, 3.0875, 3.0875, 0.69
	$L_{IRC}, W_{IRC}$	2.5, 0.7	2.5, 1	2.5, 0.9	2.5, 1.2
ZOR-3	$W, S, W_p, L$	0.585, 0.11, 1.21	0.54, 0.11, 0.95, 7.763	0.565, 0.1, 0.8, 9	0.56, 0.1, 1.1, 13.9
	$L_{s1}, L_{s2}, L_{s3}, W_s$	9.9546, 4.9773, 4.9773, 0.69	10.82, 5.14, 2.57, 0.69	12.35, 6.175, 6.175, 0.69	13.35, 6.675, 6.675, 0.69
	$L_{IRC}, W_{IRC}$	2.5, 0.7	2.5, 1	2.5, 0.9	2.5, 1.2

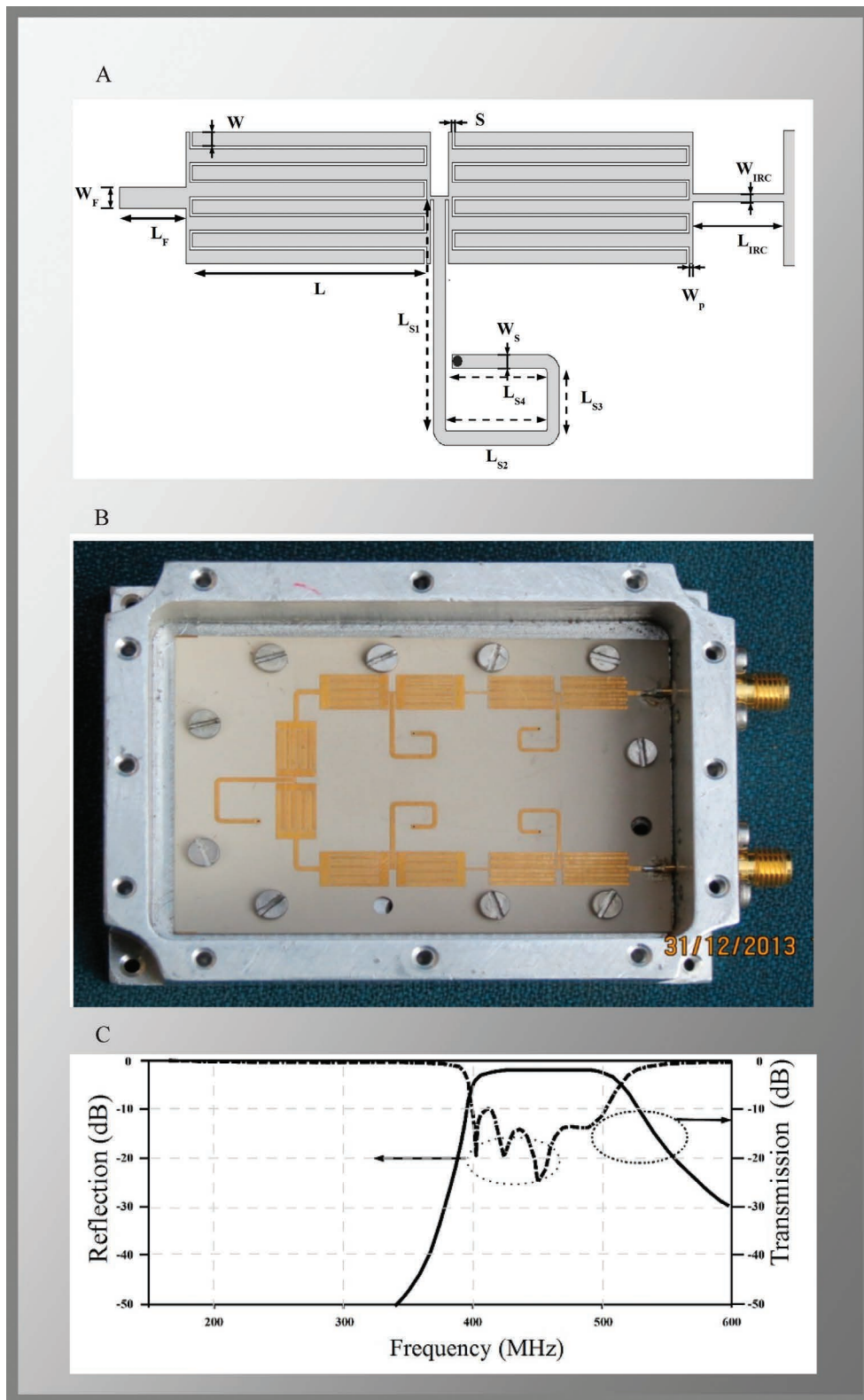


**Figure 10.** (A) Fabricated design dimension. (B) Modified fabricated design (in chassis enclosure). (C) Experimental result.

Table 5.

Measured Results for the Other Three Subbands			
Design Parameter	Achieved (Expected)	Achieved (Expected)	Achieved (Expected)
Band width(6 dB)	352–454 MHz (360–460 MHz)	311–405 MHz (300–400 MHz)	255–343 MHz (240–340 MHz)
Insertion loss	1.96 dB (400 MHz) (2.0–3.0 dB (400 MHz))	1.79 dB (350 MHz) (2.0–3.0 dB (350 MHz))	1.81 dB (290 MHz) (2.0–3.0 dB (290 MHz))

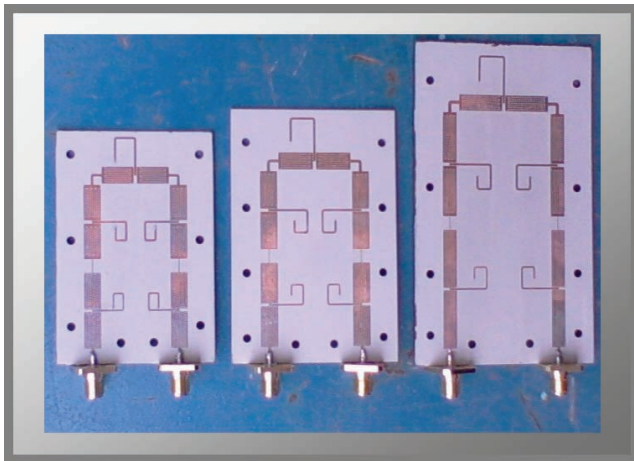


**Figure 11.** Prototypes of three MTM-ZOR filters for 360–460, 300–400, and 240–340 MHz.

allel edge-coupled filter employs the half-wavelength of a resonator. The adjacent resonators are separated by half-wavelengths. This parallel arrangement gives relatively large coupling for a given spacing between resonators, and such a structure could be used for a broadband application. Figure 13 gives a direct comparison of a coupled line filter and the MTM-ZOR filter. It shows that the MTM-ZOR filter is six times smaller than a conventional coupled line filter.

**CONCLUSION**

Employing the MTM-ZOR design resulted in a compact filter bank for a 250- to 500-MHz band of GMRT. Typically, bandwidths were in the range of 88 to 102 MHz, and the insertion loss of these filters was 1.8 to 2 dB. ♦

**ACKNOWLEDGMENTS**

We are thankful to the dean of GMRT, Prof. Y. Gupta, and the center director of National Centre for Radio Astrophysics–Tata Institute of Fundamental Research, Prof. S. K. Ghosh, for their support and encouragement for this work. Special thanks to G. Sankar, senior engineer of GMRT, for polishing the manuscript. Also thanks to Mr. Pratik Khorana, Keysight Design Engineer, for his ADS software support.

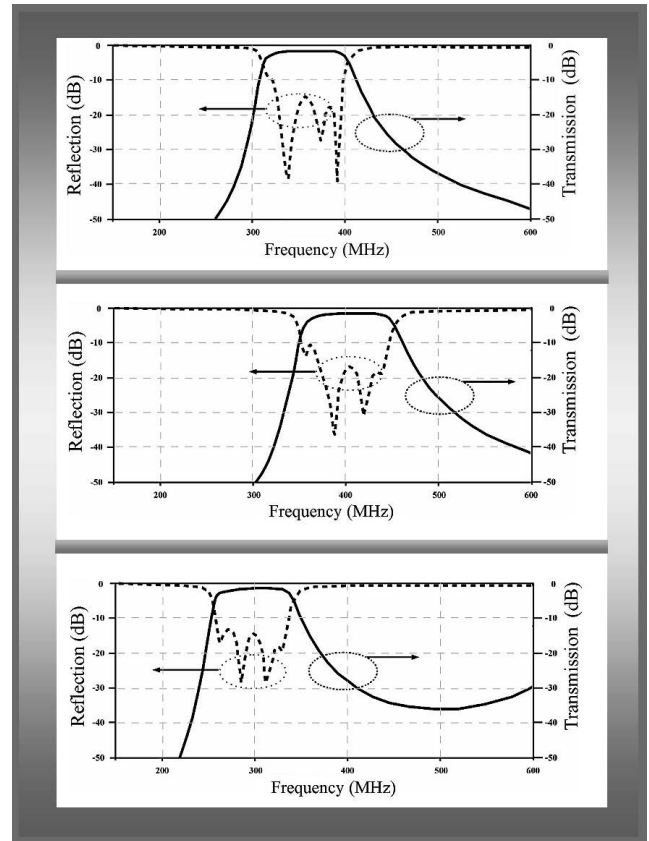


**Figure 12.** Measured results of MTM-ZOR filters for (A) 360–460 MHz, (B) 300–400 MHz, and (C) 240–340 MHz.

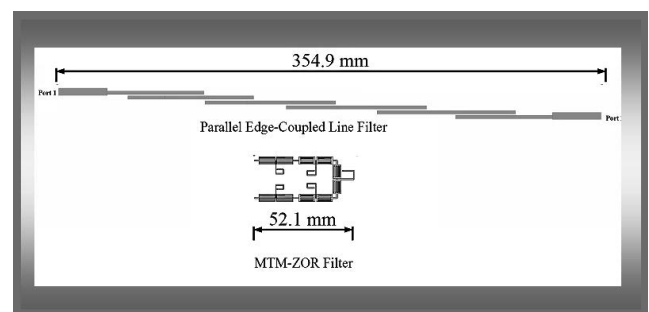


**Figure 13.** Comparison of coupled line filter and proposed MTM-ZOR filter.

## REFERENCES

- [1] Veselago, V. G. The electrodynamics of substances with simultaneously negative values of  $\epsilon$  and  $\mu$ . *Uspekhi Fizicheskikh Nauk*, Vol. 92 (July 1964), 517–526.
- [2] Caloz, C., and Itoh, T. Left-handed transmission lines and equivalent metamaterials for microwave and millimeter-wave applications. Presented at the European Microwave Conference (EuMC), Milan, Italy, Dec. 23, 2002.
- [3] Sanada, A., Caloz, C., and Itoh, T. Novel zeroth-order resonance in composite right/left handed transmission line resonators. Presented at the Asia-Pacific Microwave Conference, Seoul, Korea, Nov. 4–7, 2003.
- [4] Jang, G., and Kahng, S. Compact metamaterial zeroth-order resonator bandpass filter for a UHF band and its stopband improvement by transmission zeros. *IET Microwaves, Antennas & Propagation*, Vol. 5, 10 (July 2011), 1175–1181.
- [5] Gong, J.-Q., and Chu, Q.-X. Miniaturized microstrip bandpass filter using coupled SCRLH zeroth-order resonators. In *Proceedings of the 39th European Microwave Conference*, Rome, Italy, 2009.
- [6] Naga Satish, G., Srivastava, K. V., Biswas, A., and Kettle, D. Narrow bandpass filter using symmetrical left-handed transmission line zeroth-order resonators. Presented at the German Microwave Conference, Berlin, Germany, 2010.
- [7] Jang, G., and Kahng, S. Design of a dual-band metamaterial bandpass filter using zeroth order resonance. *Progress in Electromagnetics Research C*, Vol. 12 (2010), 149–162.
- [8] Wang, H. Zhu, L., and Menzel, W. Ultra-wideband bandpass filter with hybrid microstrip/CPW structure. *IEEE Microwave and Wireless Components Letters*, Vol. 15 (Dec. 2005), 844–846.
- [9] Caloz, C., and Itoh, T. *Electromagnetics Metamaterial: Transmission Line Theory and Microwave Application*. New York: Wiley-Interscience, John-Wiley & Sons.
- [10] Swarup G., Ananthakrishnan, S., Kapahi, V. K., Rao, A. P., Subramanya, C. R., and Kulkarni, V. K. Giant meterwave radio telescope. *Current Science*, Vol. 602 (1991).
- [11] Raut, A., Bhalerao, V., Praveen, A. P. Front-end electronics for the upgrade GMRT. *IOP Conference Series: Material Science and Engineering*. [Online] Vol. 44 (2013), 012025. Available: <http://dx.doi.org/10.1088/1757-899X/44/1/012025>.